

## CRYSTAL STRUCTURE REFINEMENT OF THE SmPd<sub>3</sub>In<sub>2</sub> COMPOUND

Yu. Tyvanchuk<sup>1\*</sup>, A. Oliynyk<sup>2</sup>, Ya. Galadzhun<sup>1</sup>,  
V. Svitlyk<sup>3</sup>, Ya. Soyka<sup>1</sup>, Ya. Kalychak<sup>1</sup>

<sup>1</sup>*Ivan Franko National University of Lviv,  
Kyryla i Mefodiya Str., 6, 79005 Lviv, Ukraine;*

<sup>2</sup>*Department of Chemistry, Hunter College, City University of New York,  
10065 New York, United States;*

<sup>3</sup>*ESRF, European Synchrotron Radiation Facility,  
Cedex, 9, 38043 Grenoble, France  
\*e-mail: yuriy.tyvanchuk@lnu.edu.ua*

The SmPd<sub>3</sub>In<sub>2</sub> compound was synthesized from the elements by arc-melting followed by annealing at 870 K. The crystal structure was refined from powder synchrotron X-ray diffraction. It crystallizes with the CePd<sub>3</sub>In<sub>2</sub>-type structure, space group *Pnma*,  $a = 10.2859(13)$ ,  $b = 4.5865(4)$ ,  $c = 9.7474(12)$  Å,  $Z = 4$ ,  $R_f = 2.56\%$ ,  $R_{\text{Bragg}} = 3.74\%$ . The refined lattice parameters of the SmPd<sub>3</sub>In<sub>2</sub> compound are the smallest in the REPd<sub>3</sub>In<sub>2</sub> series, where *RE* = La, Ce, Pr, Nd, and Sm. The structure is two-layered along the shortest cell parameter and contains chains of octahedral voids [E Sm<sub>2</sub>Pd<sub>2</sub>In<sub>2</sub>] extended along the [010] direction.

The crystal structure of the SmPdIn compound (the ZrNiAl-type structure, space group *P-62m*,  $a = 7.6596(10)$ ,  $c = 3.9366(6)$  Å,  $Z = 3$ ,  $R_f = 2.91\%$ ,  $R_{\text{Bragg}} = 5.05\%$ ), which is in equilibrium with SmPd<sub>3</sub>In<sub>2</sub>, was also refined.

**Keywords:** samarium, palladium, indium, intermetallics, crystal structure.

DOI: <https://doi.org/10.30970/vch.6601.033>

### 1. Introduction

The *RE*–Pd–In ternary systems, where *RE* stands for rare-earth elements, have attracted broad interest in recent years due to the wide variety of stoichiometry of existing ternary compounds and their physical properties. Best examples are well-known cerium-based heavy-fermion antiferromagnets CePdIn [1] and Ce<sub>8</sub>Pd<sub>24</sub>In [2], or heavy-fermion superconductors Ce<sub>2</sub>PdIn<sub>8</sub> [3] and Ce<sub>3</sub>PdIn<sub>11</sub> [4]. The isothermal sections of the Ce–Pd–In phase diagram at 1023 K [5] and the Yb–Pd–In phase diagram at 873 K [6] have been reported in the whole concentration ranges. Meanwhile, the isothermal sections of the Tb–Pd–In and Ho–Pd–In phase diagrams at 1023 K have been constructed partially around the *RE*<sub>2</sub>Pd<sub>2</sub>In compounds and along the 50 at. % Pd iso-concentration line [7]. Ternary systems with other rare earths have been studied to search for new representatives of known structure types.

According to Ref. [5], few ternary compounds have been found to exist in the Pd-rich corner of the Ce–Pd–In system:  $\text{Ce}_3\text{Pd}_{24}\text{In}$ ,  $\text{CePd}_2\text{In}$ ,  $\text{Ce}_4\text{Pd}_7\text{In}_3$ ,  $\text{CePd}_3\text{In}_2$  at 1023 K [5] where last two phases have been reported with unknown structures.

Using the single-crystal XRD method, the authors of [8] revealed that the  $\text{CePd}_3\text{In}_2$  compound crystallizes with a new structure type. The formation of the isostructural  $\text{LaPd}_3\text{In}_2$  phase has been established by the powder X-ray diffraction (XRD) method [9]. The  $\text{CePd}_3\text{In}_2$  compound has been reported as an antiferromagnet below  $T_N = 2.1$  K, and the  $\text{LaPd}_3\text{In}_2$  compound, in turn, is a Pauli paramagnet [9].

New representatives of the  $RE\text{Pd}_3\text{In}_2$  compounds with the  $\text{CePd}_3\text{In}_2$ -type structure have been reported recently [10]. The crystal structures of the compounds with  $RE = \text{Pr}$  and  $\text{Nd}$  have been solved from X-ray single crystal diffraction data, while the structure type has been assigned and the cell parameters have been determined for the compounds with  $RE = \text{La}$  and  $\text{Sm}$  based on Guinier X-ray powder diffraction patterns. We observed the formation of the  $\text{SmPd}_3\text{In}_2$  compound while studying the Sm–Pd–In ternary system at 870 K, and in this paper we report the results of complete structure determination from the synchrotron X-ray powder diffraction data.

## 2. Experimental Section

A sample with a total weight of about 1 g was arc-melted under a pure argon atmosphere on a water-cooled copper hearth. Argon was purified by a preliminary melting titanium sponge. Given the possible losses of samarium and indium during synthesis, the initial composition of the sample  $\text{Sm}_{20}\text{Pd}_{45}\text{In}_{35}$  was slightly different from the ideal 1:3:2 atomic ratio, *i.e.*  $\text{Sm}_{16.7}\text{Pd}_{50}\text{In}_{33.3}$ . Ingots of samarium of purity not lower than 99.8 wt. %, palladium 99.9 wt. %, and indium 99.99 wt. % were used as the starting materials. The sample was turned over and remelted two times to achieve homogeneity. The weight loss after the arc-melting procedure was smaller than 1 wt. %. The sample was sealed in an evacuated silica tube, annealed at 870 K for two months, and subsequently quenched in cold water.

The annealed sample was polished and semi-quantitatively investigated by EDX analyses using a REMMA-102-02 scanning electron microscope. Its phase composition was determined, and no impurity elements were detected.

Unfortunately, no single crystals suitable for crystal structure investigations were found in the ingot and annealed sample.

Powder diffraction data of the  $\text{Sm}_{20}\text{Pd}_{45}\text{In}_{35}$  sample were obtained at room temperature using a PANalytical X'Pert PRO diffractometer (Cu  $\text{K}\alpha$  radiation, Bragg-Brentano geometry, measured angle interval  $2\theta = 10\text{--}90^\circ$ , step scan mode, step size in  $2\theta = 0.03^\circ$ , 30 s per step). Because of severe absorption effects caused by the high Pd content in the sample, the XRD patterns generally suffered from weak peak intensities and high backgrounds. Therefore, further analysis of the  $\text{Sm}_{20}\text{Pd}_{45}\text{In}_{35}$  sample was carried out using synchrotron radiation. Powder XRD patterns were collected at the Canadian Light Source (Saskatoon, Canada) on the Canadian Macromolecular Crystallography Facility 08B1-1 beamline, 28 which is equipped with a Si(111) double-crystal monochromator and a two-dimensional Rayonix MX300HE detector with an active area of  $300 \times 300 \text{ mm}^2$ . The data were collected with a wavelength of  $\lambda = 0.6887 \text{ \AA}$  and a sample distance of 150 mm. Phase analysis and Rietveld refinements were carried out using the FullProf program package [11].

### 3. Results and discussion

At first, the annealed  $\text{Sm}_{20}\text{Pd}_{45}\text{In}_{35}$  sample was examined in detail by metallographic analysis. Scanning electron microscopy revealed two phases with detected compositions  $\text{Sm}_{18.7}\text{Pd}_{48.3}\text{In}_{33.0}$  (major dark phase) and  $\text{Sm}_{32.1}\text{Pd}_{35.4}\text{In}_{32.5}$  (minor light phase) in the alloy. The scanning electron micrograph is presented in Fig. 1.

The phase analysis of the annealed sample confirmed the presence of two phases (Fig. 2):  $\text{SmPd}_3\text{In}_2$  (the  $\text{CePd}_3\text{In}_2$ -type structure, space group  $Pnma$ ) and  $\text{SmPdIn}$  (the  $\text{ZrNiAl}$ -type structure, space group  $P-62m$ ). Therefore, the dark phase in the micrograph (Fig. 1) corresponds to the  $\text{SmPd}_3\text{In}_2$  compound, and the light phase is the  $\text{SmPdIn}$  compound.

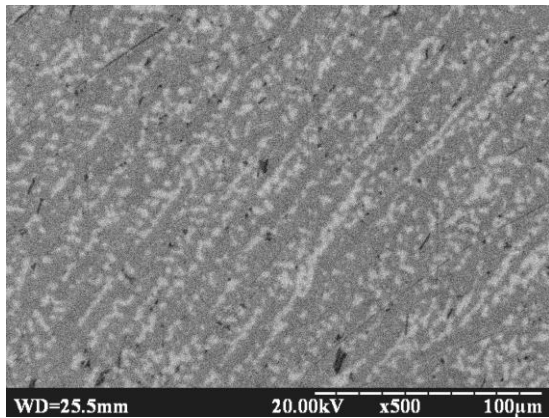


Fig. 1. Scanning electron micrograph of the  $\text{Sm}_{20}\text{Pd}_{45}\text{In}_{35}$  sample (annealed at 870 K for 2 months):  
Two phases are present in the sample:  $\text{Sm}_{18.7}\text{Pd}_{48.3}\text{In}_{33.0}$  (the  $\text{SmPd}_3\text{In}_2$  compound, dark phase)  
and  $\text{Sm}_{32.1}\text{Pd}_{35.4}\text{In}_{32.5}$  (the  $\text{SmPdIn}$  compound, light phase)

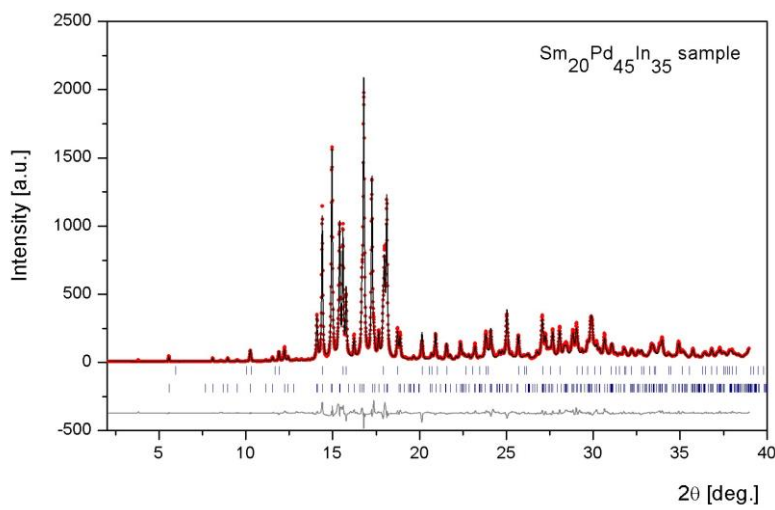


Fig. 2. Rietveld refinement (line) of the synchrotron powder XRD pattern (dots)  
and the difference curve (bottom line) for the  $\text{Sm}_{20}\text{Pd}_{45}\text{In}_{35}$  sample. The vertical bars indicate the  
positions of the Bragg reflections for the  $\text{SmPdIn}$  (upper row) and  $\text{SmPd}_3\text{In}_2$  (lower row) compounds

The experimental details of the structural refinements on powder synchrotron XRD data obtained from the annealed  $\text{Sm}_{20}\text{Pd}_{45}\text{In}_{35}$  sample are presented in Table 1. The respective diffraction pattern is shown in Fig. 2. The refined atomic coordinates and the displacement parameters for the  $\text{SmPd}_3\text{In}_2$  and  $\text{SmPdIn}$  compounds are listed in Table 2. It was found that the  $\text{Sm}_{20}\text{Pd}_{45}\text{In}_{35}$  sample contains 78(1) wt. % of the  $\text{SmPd}_3\text{In}_2$  phase and 22(1) wt. % of the  $\text{SmPdIn}$  phase.

Table 1  
Experimental details and crystallographic data for  $\text{SmPd}_3\text{In}_2$  and  $\text{SmPdIn}$   
(in the  $\text{Sm}_{20}\text{Pd}_{45}\text{In}_{35}$  sample)

Compound	$\text{SmPd}_3\text{In}_2$	$\text{SmPdIn}$
Structure type	$\text{CePd}_3\text{In}_2$	$\text{ZrNiAl}$
Space group, No	$Pnma$ , 62	$P-62m$ , 189
$Z$	4	3
Pearson's symbol	oP24	hP9
Fraction in the sample [wt. %]	78.1(8)	22.0(4)
Lattice parameters:		
$a$ , Å	10.2859(13)	7.6596(10)
$b$ , Å	4.5865(4)	
$c$ , Å	9.7474(12)	3.9366(6)
$V$ , Å <sup>3</sup>	459.85(12)	200.01(5)
Calculated density [g/cm <sup>3</sup> ]	10.100	9.256
Diffractometer, radiation		synchrotron, $\lambda = 0.6887$ Å
$2\theta$ range [deg]		2.00–38.99
Step size in $2\theta$ [deg]		0.01
$R_p$ , $R_{wp}$ , $\chi^2$		7.17, 9.70, 5.71
$R_{\text{Bragg}}$ , $R_f$	3.74, 2.56	5.05, 2.91

Table 2  
Atomic coordinates and isotropic displacement parameters for  $\text{SmPd}_3\text{In}_2$  (structure type  $\text{CePd}_3\text{In}_2$ , space group  $Pnma$ ) and  $\text{SmPdIn}$  (structure type  $\text{ZrNiAl}$ , space group  $P-62m$ )

Atom	Wyckoff position	$x$	$y$	$z$	$B_{\text{iso}}$ , Å <sup>2</sup>
$\text{SmPd}_3\text{In}_2$					
Sm	4c	0.229(1)	1/4	0.050(1)	0.9(2)
Pd1	4c	0.126(1)	1/4	0.354(2)	0.8(4)
Pd2	4c	0.242(2)	1/4	0.754(1)	1.3(4)
Pd3	4c	0.474(1)	1/4	0.603(2)	1.2(4)
In1	4c	0.015(1)	1/4	0.615(1)	0.7(3)
In2	4c	0.398(1)	1/4	0.334(1)	1.0(3)
$\text{SmPdIn}$					
Sm	3f	0.588(1)	0	0	1.1(3)
Pd1	1a	0	0	0	1.0(6)
Pd2	2d	1/3	2/3	1/2	2.0(9)
In	3g	0.254(2)	0	1/2	0.7(4)

All atomic sites in the  $\text{SmPd}_3\text{In}_2$  and  $\text{SmPdIn}$  structures are fully occupied by one type of atom, *i.e.*, no traces of atomic mixtures or deficiencies were detected. A projection of the unit cell onto the  $XZ$  plane and the coordination polyhedra of the atoms of  $\text{SmPd}_3\text{In}_2$  are shown in Fig. 3. Interatomic distances compared to the sum of the respective atomic radii [12] and the coordination numbers of atoms in the  $\text{SmPd}_3\text{In}_2$  compound are provided in Table 3. Samarium, indium, and palladium atoms have coordination polyhedra in the form of pentagonal, tetragonal, and trigonal prisms with additional atoms, respectively.

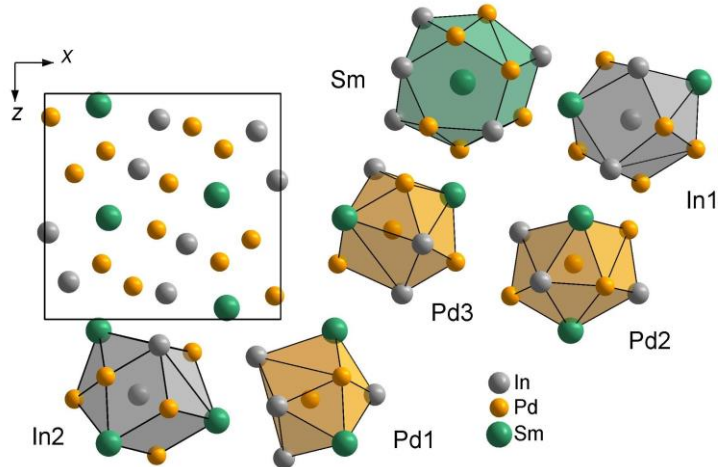


Fig. 3. Projection of the unit cell of  $\text{SmPd}_3\text{In}_2$  onto the  $XZ$  plane and coordination polyhedra of the atoms

Table 3  
Interatomic distances ( $d$ ),  $\Delta$  values ( $\Delta = 100(d - \Sigma r)/\Sigma r$ , where  $\Sigma r$  is the sum of the respective atomic radii [12]) and atomic coordination numbers (CN) for  $\text{SmPd}_3\text{In}_2$ .

Standard deviations of  $d$  are equal to or smaller than  $0.005 \text{ \AA}$

Atom		$d, \text{ \AA}$	$\Delta, \%$	Atom		$d, \text{ \AA}$	$\Delta, \%$		
Sm	Pd2	1x	2.890	-9.0	Pd3	In2	2x	2.710	-9.7
	Pd3	1x	3.015	-5.1	In2	1x	2.737	-8.8	
	Pd2	2x	3.049	-4.0	CN = 11	In1	1x	2.776	-7.5
	Pd1	1x	3.140	-1.2	Pd2	1x	2.811	2.1	
	Pd3	2x	3.145	-1.0	Sm	1x	3.015	-5.1	
	In2	1x	3.271	-4.5	Pd2	1x	3.078	11.8	
	Pd1	2x	3.345	5.3	Pd3	2x	3.098	12.6	
	In1	1x	3.355	-2.1	Sm	2x	3.145	-1.0	
	In2	2x	3.377	-1.5	In1	Pd2	1x	2.699	-10.1
	In1	2x	3.553	3.6	Pd1	2x	2.726	-9.2	
CN = 16	In2	1x	3.5794	4.4	CN = 13	Pd3	1x	2.776	-7.5
	Pd1	In1	2x	2.726	Pd1	1x	2.791	-7.0	
	In1	1x	2.791	-7.0	Pd2	1x	3.086	2.8	
	CN = 10	In2	1x	2.812	In1	2x	3.221	-0.9	
	Pd2	2x	2.841	3.2	In2	2x	3.260	0.3	
	In2	1x	2.969	-1.1	Sm	1x	3.355	-2.1	
	Sm	1x	3.140	-1.2	Sm	2x	3.553	3.6	
CN = 11	Sm	2x	3.345	5.3	In2	Pd3	2x	2.710	-9.7
	Pd2	In1	1x	2.699	Pd3	1x	2.737	-8.8	
	Pd3	1x	2.811	2.1	CN = 13	Pd1	1x	2.812	-6.3
	In2	2x	2.817	-6.2	Pd2	2x	2.817	-6.2	
	Pd1	2x	2.841	3.2	Pd1	1x	2.969	-1.1	
	Sm	1x	2.890	-9.0	In1	2x	3.260	0.3	
	Sm	2x	3.049	-4.0	Sm	1x	3.271	-4.6	
In1	Pd3	1x	3.078	11.8	Sm	2x	3.377	-1.5	
	In1	1x	3.086	2.8	Sm	1x	3.579	4.4	

So far, only structure type and cell parameters have been published for the SmPdIn compound [13], while its physical properties have been studied in detail [14]. Therefore, the refined atomic coordinates of SmPdIn are reported for the first time.

#### 4. Conclusion

The investigated compound, evidently, completes the  $REPd_3In_2$  series because the concerned  $RE_{16.7}Pd_{50}In_{33.3}$  composition with the heavy rare earths Tb, Ho, and Yb [6, 7] corresponds to the solid solution  $RE_xPdIn_{1-x}$  based on the PdIn binary compound. The refined lattice parameters of the SmPd<sub>3</sub>In<sub>2</sub> compound are the smallest in the  $REPd_3In_2$  series and agree well with the results of Ref. [10].

As shown in Fig. 1 of Ref. [8], rare earth atoms are located in the pentagonal channels along the [010] direction in the  $REPd_3In_2$  structure.

The  $REPd_3In_2$  compounds belong to the second group of  $RE-T-In$  compounds ( $T$  stands for transition metal), according to the review article [15]. These are usually two-layered structures along the shortest cell parameter ( $\sim 4.5$  Å) with average values of the coordination numbers of atoms. Along the  $Y$  axis, their structure contains chains of octahedral voids  $[E Sm_2Pd_2In_2]$ , which connect each other with faces and extend along the [010] direction (Fig. 4). Since these chains contain rare earth atoms, the transition from Sm to La will change their geometry at first and most noticeably along the  $Y$  axis.

Therefore, this material can be used to store small atoms (molecules), such as hydrogen. Similar chains of empty octahedra  $[E Ni_2In_4]$  are reported for  $LaNi_3In_6$ -type compounds [16], while isolated octahedra  $[E RE_6]$  were found for  $RE_{23}Ni_7In_4$  [17].

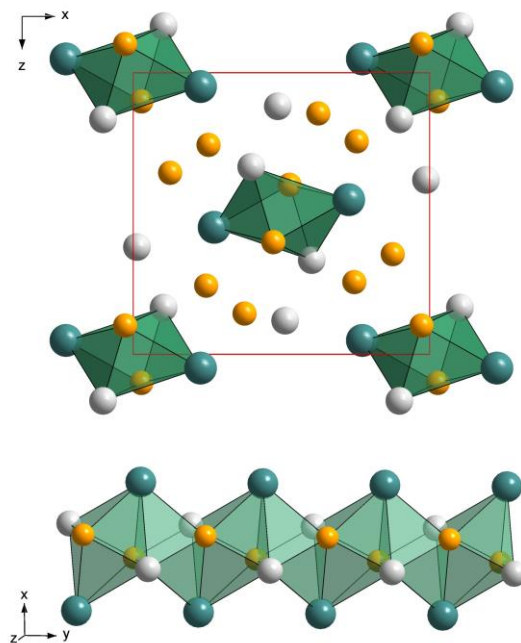


Fig. 4. Empty octahedra  $[E Sm_2Pd_2In_2]$  in the  $SmPd_3In_2$  structure

## 5. Acknowledgments

The authors thank Dr. R. Ya. Serkiz (Laboratory of Low Temperature Investigations, Ivan Franko National University of Lviv) for collecting SEM/EDX data.

Yu. Tyvanchuk and Ya. Kalychak gratefully acknowledge partial support of this research by the Simons Foundation (SFI-PD-Ukraine-00014574).

1. *Kurisu M., Takabatake T., Fujii H.* High-pressure study on the dense Kondo system CeNiIn, CePdIn and CePtIn // *J. Magnet. Magnetic Mat.* 1990. Vol. 90–91. P. 469–470. DOI: [https://doi.org/10.1016/S0304-8853\(10\)80169-6](https://doi.org/10.1016/S0304-8853(10)80169-6)
2. *Cho B. K., Gordon R. A., W. Jones C. D., DiSalvo F. J.* et al. Specific heat and heavy-fermionic behavior in Ce<sub>8</sub>Pd<sub>24</sub>M (M = Ga, In, Sn, Sb, Pb, and Bi) // *Phys. Rev. B.* 1998. Vol. 57. P. 15191. DOI: <https://doi.org/10.1103/PhysRevB.57.15191>
3. *Kaczorowski D., Pikul A. P., Gnida D., Tran V. H.* Emergence of a Superconducting State from an Antiferromagnetic Phase in Single Crystals of the Heavy Fermion Compound Ce<sub>2</sub>PdIn<sub>8</sub> // *Phys. Rev. Lett.* 2009. Vol. 103. P. 027003. DOI: <https://doi.org/10.1103/PhysRevLett.103.027003>
4. *Kratochvilova M., Dusek M., Uhlirova K., Rudajevova A.* et al. Single crystal study of the layered heavy fermion compounds Ce<sub>2</sub>PdIn<sub>8</sub>, Ce<sub>3</sub>PdIn<sub>11</sub>, Ce<sub>2</sub>PtIn<sub>8</sub> and Ce<sub>3</sub>PtIn<sub>11</sub> // *J. Crystal Growth.* 2014. Vol. 397. P. 47–52. DOI: <https://doi.org/10.1016/j.jcrysGro.2014.04.008>
5. *Giovannini M., Saccone A., Delfino S., Rogl P., Ferro R.* The isothermal section at 750° C of the Ce–Pd–In system // *Intermetallics.* 2003. Vol. 11. P. 197–206. DOI: [https://doi.org/10.1016/S0966-9795\(02\)00185-1](https://doi.org/10.1016/S0966-9795(02)00185-1)
6. *Akbar F., Martinelli A., Čurlík I., Reiffers M., Giovannini M.* Phase relations at 600° C in ytterbium-palladium-indium system // *J. Alloys Compd.* 2022. Vol. 920. P. 165882. DOI: <https://doi.org/10.1016/j.jallcom.2022.165882>
7. *Giovannini M., Saccone A., Delfino S., Rogl P.* A comparative investigation of isothermal sections of Rare Earth–Pd–In systems // *Intermetallics.* 2003. Vol. 11. P. 1237–1243. DOI: [https://doi.org/10.1016/S0966-9795\(03\)00164-X](https://doi.org/10.1016/S0966-9795(03)00164-X)
8. *Nesterenko S. N., Tursina A. I., Rogl P., Seropegin Y. D.* Single crystal investigation of CePd<sub>3</sub>In<sub>2</sub> // *J. Alloys Compd.* 2004. Vol. 373. P. 220–222. DOI: <https://doi.org/10.1016/j.jallcom.2003.11.002>
9. *Kaldarar H., Royanian E., Michor H., Hilscher G.* et al. Thermal and electronic properties of CePd<sub>3</sub>In<sub>2</sub> // *Phys. Rev. B.* 2009. Vol. 79. P. 205104. DOI: <https://doi.org/10.1103/PhysRevB.79.205104>
10. *Engelbert S., Stegemann F., Bönnighausen J., Klenner S.* et al. Intermetallics of the types REPd<sub>3</sub>X<sub>2</sub> and REPt<sub>3</sub>X<sub>2</sub> (RE = La–Nd, Sm, Gd, Tb; X = In, Sn) with substructures featuring tin and In atoms in distorted square-planar coordination // *Z. Naturforsch. B.* 2019. Vol. 74. P. 865–878. DOI: <https://doi.org/10.1515/znb-2019-0166>
11. *Rodriguez–Carvajal J.* Recent developments of the program FULLPROF // *Commission on Powder Diffraction (IUCr). Newsletter.* 2001. Vol. 26. P. 12–19.
12. *Emsley J.* The Elements. 2nd ed. Oxford: Clarendon Press, 1991. 251 p.
13. *Ferro R., Marazza R., Rambaldi G.* Equiatomic Ternary Phases in the Alloys of the Rare Earths with Indium and Nickel or Palladium // *Z. Metallkd.* 1974. Vol. 65. P. 37–39.
14. *Ito T., Ohkubo K., Hirasawa T., Takeuchi J., Hiromitsu I., Kurisu M.* Magnetic properties of SmPdIn single crystals // *J. Magn. Magn. Mater.* 1995. Vol. 140–144. P. 873–874.

15. *Kalychak Ya. M., Zaremba V. I., Pöttgen R., Lukachuk M., Hoffmann R.-D.* Rare Earth–Transition Metal–Indides // In: K. A. Gschneidner, Jr., J.-C. Bünzli, V. K. Pecharsky (Eds.). *Handbook on the Physics and Chemistry of Rare Earths*. Elsevier; Amsterdam, 2004. Vol. 34. P. 1–133. DOI: [https://doi.org/10.1016/S0168-1273\(04\)34001-8](https://doi.org/10.1016/S0168-1273(04)34001-8)
16. *Kalychak Y. M., Gladyshevskii E. I., Bodak O. I., Dmytrakh O. V., Kotur B. Y.* Crystal structure of  $\text{LaNi}_3\text{In}_6$ ,  $\text{CeNi}_3\text{In}_6$ , and  $\text{PrNi}_3\text{In}_6$  // Sov. Phys. Crystallogr. 1985. Vol. 30. P. 344–345.
17. *Tyvanchuk Yu. B., Fecica M., Garcia G., Mar A., Oliynyk A. O.* Ternary rare-earth–metal nickel indides  $RE_{23}\text{Ni}_7\text{In}_4$  ( $RE = \text{Gd, Tb, Dy}$ ) with  $\text{Yb}_{23}\text{Cu}_7\text{Mg}_4$ -type structure // Inorg. Chem. 2021. Vol. 60, Iss. 23. P. 17900–17910. DOI: <https://doi.org/10.1021/acs.inorgchem.1c02486>

## УТОЧНЕННЯ КРИСТАЛІЧНОЇ СТРУКТУРИ СПОЛУКИ $\text{SmPd}_3\text{In}_2$

**Ю. Тиванчук<sup>1\*</sup>, А. Олійник, Я. Галаджун<sup>1</sup>, В. Світлик<sup>3</sup>, Я. Сойка<sup>1</sup>, Я. Каличак<sup>1</sup>**

<sup>1</sup>Львівський національний університет імені Івана Франка,  
бул. Кирила і Мефодія, 6, 79005 Львів, Україна;

<sup>2</sup>Хімічний факультет, Коледж Гантера, Міський університет Нью-Йорка,  
10065 Нью-Йорк, США;

<sup>3</sup>Європейський центр синхротронного випромінювання,  
Цедекс, 9, 38043 Гренобль, Франція  
\*e-mail: [yuriy.tyvanchuk@lnu.edu.ua](mailto:yuriy.tyvanchuk@lnu.edu.ua)

Зразок для дослідження  $\text{SmPd}_3\text{In}_2$  синтезовано електродуговим плавленням шихти металів чистотою не менше 99,8 мас. % основного компонента і відпалено при 870 К у вакуумованій кварцовій ампулі упродовж двох місяців. Для запобігання втратам самарію та індію початковий склад зразка становив  $\text{Sm}_{20}\text{Pd}_{45}\text{In}_{35}$ , замість  $\text{Sm}_{16,7}\text{Pd}_{50}\text{In}_{33,3}$ .

Масиви дифракційних даних отримано з використанням дифрактометра PANalytical X'Pert PRO (Cu K $\alpha$ -випромінювання). Через сильне поглинання, спричинене високим вмістом Pd у зразку, рентгенограми мали слабкі піки інтенсивностей та високий фон. Тому подальший аналіз зразка  $\text{Sm}_{20}\text{Pd}_{45}\text{In}_{35}$  проводили з використанням синхротронного випромінювання за довжини хвилі  $\lambda = 0,6887$  Å (Canadian Macromolecular Crystallography Facility 08B1-1 beamline 28). Фазовий аналіз та уточнення структури методом Рітвельда проводили за допомогою програмного пакета FullProf.

Структура сполуки  $\text{SmPd}_3\text{In}_2$  належить до типу  $\text{CePd}_3\text{In}_2$ , просторова група  $Pnma$ ,  $a = 10,2859(13)$ ,  $b = 4,5865(4)$ ,  $c = 9,7474(12)$  Å,  $Z = 4$ ,  $R_f = 2,56\%$ ,  $R_{\text{Bragg}} = 3,74\%$ . Також уточнено кристалічну структуру сполуки  $\text{SmPdIn}$  (тип  $\text{ZrNiAl}$ , просторова група  $P-62m$ ,  $a = 7,6596(10)$ ,  $c = 3,9366(6)$  Å,  $Z = 3$ ,  $R_f = 2,91\%$ ,  $R_{\text{Bragg}} = 5,05\%$ ), яка перебуває у рівновазі з  $\text{SmPd}_3\text{In}_2$ . У сполуках  $\text{SmPd}_3\text{In}_2$  і  $\text{SmPdIn}$  усі сорти атомів упорядковано займають відповідні правильні системи точок, тобто ми не виявили суміші атомів або дефектності структур.

Уточнені параметри комірки  $\text{SmPd}_3\text{In}_2$  є найменшими в ряді  $RE\text{Pd}_3\text{In}_2$ , де  $RE = \text{La, Ce, Pr, Nd}$  і  $\text{Sm}$ . Структура є двошаровою у напрямку найкоротшого параметра комірки і містить ланцюжки октаедричних пустот  $[\text{E Sm}_2\text{Pd}_2\text{In}_2]$ , витягнуті вздовж напрямку [010].

**Ключові слова:** самарій, паладій, індій, інтерметаліди, кристалічна структура.

Стаття надійшла до редколегії 30.10.2024  
Прийнята до друку 21.01.2025